Journal of Hydroinformatics

Journal of Hydroinformatics Vol 00 No 0, 1 doi: 10.2166/hydro.2024.041

Improving incomplete mixing modeling for junctions of water distribution networks

Reza Yousefian * and Sophie Duchesne

Institut national de la recherche scientifique, Centre Eau Terre Environnement, 490, rue de la Couronne, Québec, QC G1K 9A9, Canada
*Corresponding author. E-mail: reza.yousefian@inrs.ca

RY, 0000-0003-0442-8816; SD, 0000-0002-5619-0849

ABSTRACT

Most of the existing water quality models for water distribution networks assume complete mixing at junctions. Albeit few models offer the possibility to consider incomplete mixing (IM) at junctions, most of them were developed under laboratory conditions and for equal pipe size junctions. In real-world distribution networks, however, cross junctions of $150 \times 100 \times 150 \times 100$ mm or $100 \times 150 \times 150 \times 150$ mm are common, yet no model has been developed for these configurations. This paper presents a new equation to compute concentrations in cross junction outlets while considering IM for six cross junction configurations, including unequal pipe sizes and 150 mm pipes. For each cross junction configuration, mixing was studied under 25 flow scenarios in the laboratory and 40 simulated flow scenarios using OpenFOAM software. Two new flow rate ratios were selected as independent variables to compute different outlet concentrations. For two specific cross junctions with equal pipe sizes, the root-mean-squared error between the observed and simulated concentrations of the newly developed model was 0.02, while it was 0.05 and 0.07, respectively, for the AZRED IM model and the Shao *et al*. IM model.

Key words: computational fluid dynamics, incomplete mixing, OpenFOAM, twoLiquidMixingFoam, water distribution networks, water quality models

HIGHLIGHTS

- Laboratory experiments were conducted under real-world conditions with 150 mm pipes.
- New principal combinations of independent variables for mixing were identified.
- A single equation was developed for mixing in different cross junction configurations.
- The developed model reproduces observations more accurately than the other models.

GRAPHICAL ABSTRACT

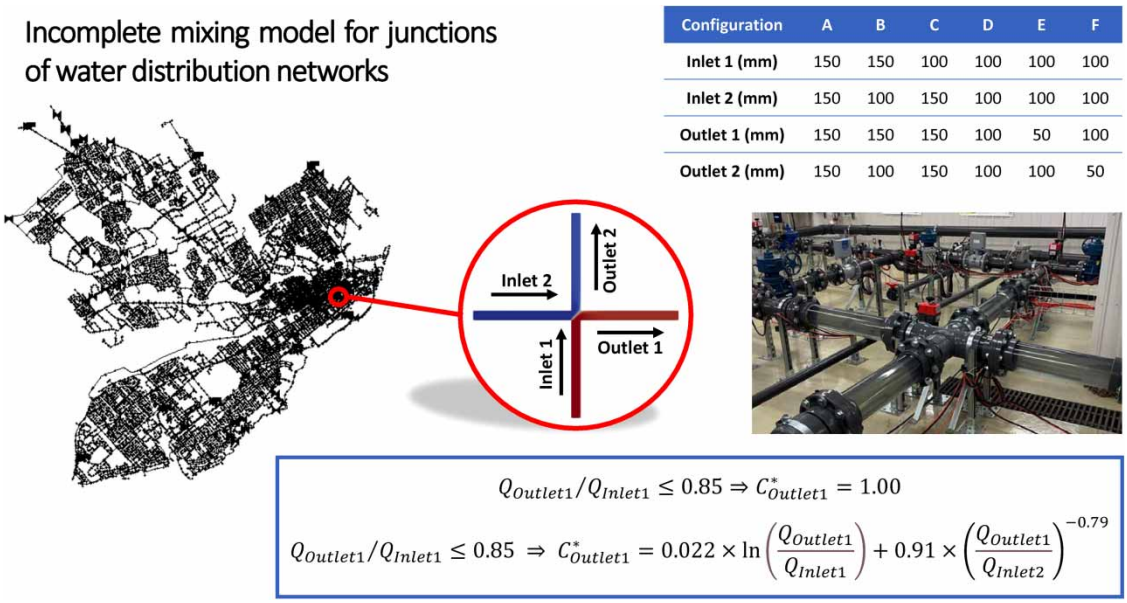

Configuration	A	B	C	D	E	F
Inlet 1 (mm)	150	150	100	100	100	100
Inlet 2 (mm)	150	100	150	100	100	100
Outlet 1 (mm)	150	150	150	100	50	100
Outlet 2 (mm)	150	100	150	100	100	50

$$Q_{Outlet1}/Q_{Inlet1} \leq 0.85 \Rightarrow C^*_{Outlet1} = 1.00$$

$$Q_{Outlet1}/Q_{Inlet1} \leq 0.85 \Rightarrow C^*_{Outlet1} = 0.022 \times \ln\left(\frac{Q_{Outlet1}}{Q_{Inlet1}}\right) + 0.91 \times \left(\frac{Q_{Outlet1}}{Q_{Inlet2}}\right)^{-0.79}$$

1. INTRODUCTION

The mixing phenomenon is increasingly recognized as a serious concern in drinking water quality models of water distribution networks (WDNs). Indeed, in most existing water quality models (such as EPANET (Environmental Protection Agency Network Evaluation Tool) (Rossman 2000) or WaterCAD (Water Computer-Aided Design)/WaterGEMS (WATER Geographic Engineering Modeling System) (Bentley Systems 2020)), the mixing of water quality constituents at junctions is simplified and considered to be complete and instantaneous, which can greatly reduce the accuracy of the predicted concentration values.

A complete mixing assumption was adopted in drinking water quality models to reduce simulation time and model complexity. The degree of mixing at junctions depends on a wide range of parameters, such as the junction type (cross or tee junction), junction configuration (e.g., junctions with different pipe diameters in their legs), and hydraulic conditions. Due to the importance of water quality models in urban WDNs and technological advances provided by high-speed computers, more accurate models have been developed within the last decades, allowing for the simulation of mixing at junctions instead of considering the simplistic assumption of complete mixing.

Fowler & Jones (1991) and Ashgriz *et al.* (2001) were among the first researchers to find that mixing should not be considered complete at the junctions of WDNs, unlike the assumption employed in most existing water quality software such as EPANET (Rossman 2000) or WaterCAD (Water Computer-Aided Design)/WaterGEMS (WATER Geographic Engineering Modeling System) (Bentley Systems 2020). Many researchers conducted laboratory studies on such a mixing phenomenon to investigate the details of mixing in cross junctions (Orear *et al.* 2005; Ho *et al.* 2006; McKenna *et al.* 2007; McKenna *et al.* 2008; Song *et al.* 2009; van Summeren *et al.* 2017; Song *et al.* 2018; Shao *et al.* 2019; Yousefian & Duchesne 2022a) or double-tee junctions (Orear *et al.* 2005; Ho *et al.* 2006; Ung *et al.* 2014; Cotes *et al.* 2016; Ung 2016; Gilbert *et al.* 2017; Song *et al.* 2018; Shao *et al.* 2019; Grbčić *et al.* 2020b). Likewise, many authors used experimental results of the mixing phenomenon at junctions to calibrate different computational fluid dynamics (CFD) tools (Orear *et al.* 2005; Webb & van Bloemen Waanders 2006; Ho *et al.* 2007; Webb 2007; Romero-Gomez *et al.* 2008c; Braun *et al.* 2015; Cotes *et al.* 2016; Hernández Cervantes *et al.* 2018; Grbčić *et al.* 2020b; Grbčić *et al.* 2020a). Alternatively, other researchers focused on the impact of the mixing phenomenon on sensor network designs, optimal sensor placements, and the distribution of disinfectants or residual chlorine in WDNs (Romero-Gomez *et al.* 2008a; Romero-Gomez & Choi 2011; Mompremier *et al.* 2015; Mompremier *et al.* 2017).

Several attempts have been made to develop different models for incomplete mixing (IM). AZRED (AZ refers to the University of Arizona, where the model was developed, and RED is a Spanish word for network) is one of the first models to

project the concentrations of solute at junction outlets (Austin *et al.* 2008; Choi *et al.* 2008). In this model, the ratio of Reynolds (Re) number in one inlet to the other inlet (inlet Re numbers ratio) and the ratio of Re number in one outlet to the other outlet (outlet Re numbers ratio) are independent variables used to compute the concentration in outlets.

EPANET-BAM (Bulk Advective Mixing) is another model for IM that originally considered only the advection term of the transport equation and neglected the effect of diffusion in mixing (Ho 2008). In this model, the solute concentration in the outlet adjacent to the inlet with a higher flow rate was considered equal to the solute concentration in the inlet with a higher flow rate. The solute concentration of the other outlet was then calculated based on the mass balance equation. Later on, a scaling parameter was added in EPANET-BAM to take into account the effect of the diffusion term in the mixing phenomenon (McKenna *et al.* 2007; Ho & Khalsa 2008; Romero-Gomez *et al.* 2008b).

Shao *et al.* (2014) developed an empirical model for IM, whereby the independent variables are the flow momentum of inlets and outlets, defined as the ratio of the squared flow rate to the pipe section area. The dependent variable of this model is a newly defined flow distribution factor employed to project the solute concentration in outlets.

Besides AZRED, EPANET-BAM, and the analytical model by Shao *et al.* (2014), others were developed specifically for cross junctions. Hernández Cervantes *et al.* (2021) proposed a new model for IM in cross junctions where the inlet flow ratio, the outlet flow ratio, and the inlet concentration ratio are used as input variables, while the ratio of concentrations in the outlets is the output. In addition, Hammoudi (2021) suggested a regression equation to estimate the mass fraction at the outlets of a cross junction based on the ratio of flows in the inlets, the ratio of flows in the outlets, the density and diffusivity of the contaminant, the pipe diameter of the cross junction, and the Re number of contaminated inlets for the mixing in WDNs.

Among the existing models, two models can be employed for junctions with two pipe sizes where the opposite legs have the same pipe size. The first of these, EPANET-BAM-WRAP, is an IM model based on EPANET that estimates the solute concentration in the outlets of the junctions with two pipe sizes (Ho & O'Rear 2009). In this model, like in EPANET-BAM, a scaling parameter is defined to consider the effect of diffusion in mixing, for each junction. The second is an analytical model by Yu *et al.* (2014b), where it is assumed that the main pipes (the inlet with the higher flow rate and the outlet opposing that inlet) have a larger pipe diameter. This model can be used for three ratios of pipe diameter (mm), namely 25/25, 25/32, and 25/50, within cross and double-tee junctions (Yu *et al.* 2014b, 2014a, 2016). In this empirical model, a new mixing index was proposed based on the conservation of flow and solute at junctions. Finally, a regression equation was employed in this model to project the mixing index as a function of the inlet pipe diameter ratio, the inlet Re number ratio, and the outlet Re number ratio.

Further details regarding the existing IM models and studies carried out on the mixing phenomenon in the junctions of WDNs can be found in Yousefian & Duchesne (2022b). This review paper revealed that most existing IM models were developed based on laboratory experiments with small pipe diameters (25–50 mm) and low pressure.

Yousefian & Duchesne (2022a) studied the impact of pressure on the mixing phenomenon and found that for pressures higher than 140 kPa, the pressure does not have a significant impact on the mixing phenomenon. Later, Yousefian (2023) investigated the accuracy of the existing IM models within laboratory experiments and showed that using the existing IM models for real-world pipe diameters (100 mm and more) can lead to erroneous results. Besides, the IM models that can work for junctions with two pipe sizes either need to be calibrated based on experimental results (e.g., EPANET-BAM-WRAP) or can only be used for three specific pipe diameter ratios (e.g., analytical model by Yu *et al.* (2014b)).

Furthermore, Yousefian & Duchesne (2022b) found that no model exists to consider IM for common junctions, such as those cross junctions with pipe diameters of $150 \times 100 \times 150 \times 100$ mm, $100 \times 150 \times 150 \times 150$ mm, or $100 \times 100 \times 50 \times 100$ mm. Therefore, the objective of this study was to develop an IM model that can be employed for cross junctions with real-world pipe diameters (e.g., 100 and 150 mm) and also for cross junctions with different pipe diameters in their legs.

2. METHODOLOGY

This study consisted of six main steps to address each challenge and difficulty of the research (see Figure 1). First, a statistical analysis of a real-world WDN in North America was conducted to provide the required data for finding the real-world conditions, including the most common junction types (cross or double-tee junction), junction sizes, junction configurations (pipe sizes in junction legs), and flow rates. A small WDN was then designed in a hydraulic laboratory based on the specifications of the real-world WDN to investigate the IM under real-world conditions, and subsequent experiments of each cross junction were conducted. Since there was a limit on the maximum flow rate in laboratory experiments 4.5 LPS (Liters Per Second), a

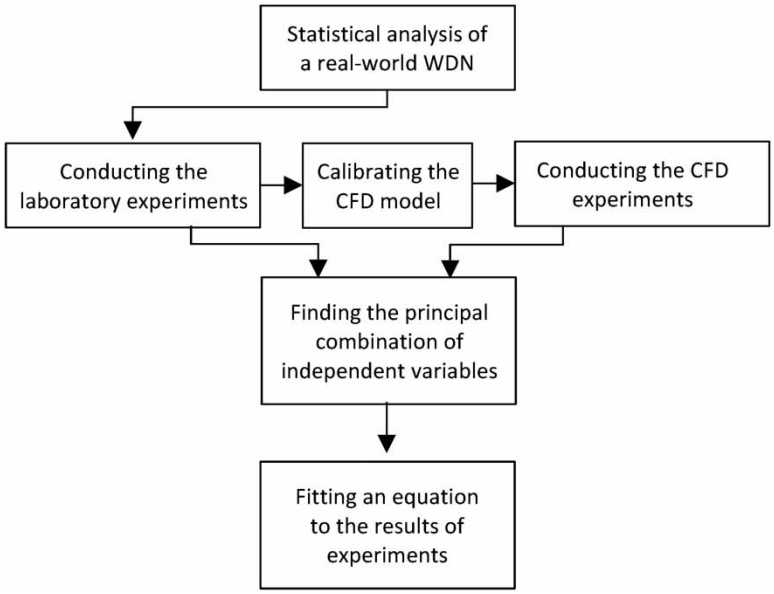

Figure 1 | Flow chart of the steps taken in the current research.

CFD model was also calibrated based on the experimental results and employed to conduct the experiments for flow rate scenarios other than those studied in the laboratory. Different combinations of independent variables were then tested to find the principal combination explaining the outlet concentrations. Finally, a single equation was derived for estimating the outlet concentrations in all studied cross junctions.

2.1. Statistical analysis of a real WDN

Among the characteristics of drinking WDNs, pipe size, and pressure are important parameters that are different between the experiments performed to develop the existing IM models and real-world conditions. Yousefian & Duchesne (2022a) recently showed that pressure cannot significantly affect mixing. However, the same authors also showed, in Yousefian (2023), that the junction size has a significant impact on the mixing behavior, when the junction size is smaller than 100 mm. In order to determine the characteristics of the experimental setup in the laboratory, the pipe and flow characteristics of a North American WDN serving a population of about one million people were investigated. To do so, the number and type of junctions with IM, the size of commonly used pipes, the configuration of junctions, and the most frequent flow rates were investigated for that WDN. The mini WDN Laboratory of Institut National de la Recherche Scientifique (INRS; see description below) was then redesigned and rebuilt based on these conditions to study the mixing behavior under real-world conditions.

The most frequent conditions of real-world WDNs were obtained from the analysis of 24-h average water demand on a normal day in the selected North American city. In this analysis, all junctions have been examined to determine if the junction is within the complete mixing conditions or not in normal flow conditions. To do so, the junctions were first divided into cross junctions and double-tee junctions. Among each type, those junctions with two inlets and two outlets were then selected. Next, those junctions with adjacent inlets were identified as junctions with IM conditions. Moreover, for double-tee junctions, those with a distance between tee junctions less than 10 diameters of the pipes were considered double-tee junctions with IM. According to such criteria, approximately 65% of the cross junctions in this WDN were within the conditions of IM, while only about 1% of its double-tee junctions had characteristics that led to IM. Besides, about 60% of the cross junctions with IM characteristics have different pipe sizes in their legs. It was also found that the most frequently used pipe sizes in this WDN were 100 and 150 mm. Therefore, based on these observations, six cross junction configurations with pipe sizes of 50, 100, and 150 mm were selected to study the mixing behavior within them. Those configurations are listed in Table 1. For cross junctions with different pipe sizes, two different types of reducers were used: a reducer coupling that gradually changes

Table 1 | Cross junction configurations tested in the laboratory

Configuration	South inlet size (salty water) (mm)	West inlet size (tap water) (mm)	North outlet size (mm)	East outlet size (mm)	Connection type
A	150	150	150	150	(–)
B	150	100	150	100	Reducer coupling
C	100	150	150	150	Reducer coupling
D	100	100	100	100	(–)
E	100	100	50	100	Reducer bushing
F	100	100	100	50	Reducer bushing

the pipe diameter from 150 to 100 mm in a length of 10 cm (configurations B and C) and a reducer bushing in which the pipe diameter suddenly reduces from 100 to 50 mm (configurations E and F).

It was observed that the flow rates between 1.50 and 3.00 LPS were the most common during a normal day in the studied WDN. Accordingly, for laboratory experiments, two series of flow scenarios were tested: the first series was used to develop a new IM model for cross junctions with different pipe sizes (Table 2) and the second series was employed to validate the new IM model (Table 3).

In addition to the flow rate scenarios tested in the laboratory (which were selected through the analysis of a real-world WDN), others were tested through CFD simulations to fill the gap between the laboratory flow scenarios and some extreme flow rate scenarios observed in the real-world WDN. The flow rate scenarios selected for the CFD experiments are shown in Table 3.

2.2. Experimental setup

Laboratory experiments were carried out in the Mini Water Distribution Network Laboratory of Institut National de la Recherche Scientifique (INRS) in Quebec City, Canada. The network is equipped with two pumps: a 3 hp pump (Xylem-AquaBoost) and a 75 hp pump (Berkeley-B4EPBMS). Twelve flow control valves with electric actuators (Assured Automation-P2R4 with S4 actuator) were installed to apply a variety of pressure and flow configurations. The pressures in the network were measured with six pressure probes (Ashcroft-G2) and the flow rates were measured by nine electromagnetic flow meters (ModMAG-M2000) (Figure 2(a)). The soluble tracer for laboratory experiments was sodium chloride (NaCl),

Table 2 | Laboratory flow rate scenarios for developing the new IM model

Scenario	South inlet (salty water) (LPS)	West inlet (tap water) (LPS)	North outlet (LPS)	East outlet (LPS)
Lab-1	1.50	3.00	3.00	1.50
Lab-2	1.50	3.00	2.50	2.00
Lab-3	1.50	3.00	2.25	2.25
Lab-4	1.50	3.00	2.00	2.50
Lab-5	1.50	3.00	1.50	3.00
Lab-6	2.25	2.25	3.00	1.50
Lab-7	2.25	2.25	2.50	2.00
Lab-8	2.25	2.25	2.25	2.25
Lab-9	2.25	2.25	2.00	2.50
Lab-10	2.25	2.25	1.50	3.00
Lab-11	3.00	1.50	3.00	1.50
Lab-12	3.00	1.50	2.50	2.00
Lab-13	3.00	1.50	2.25	2.25
Lab-14	3.00	1.50	2.00	2.50
Lab-15	3.00	1.50	1.50	3.00

Table 3 | Laboratory flow rate scenarios for validating the new IM model

Scenario	South inlet (salty water) (LPS)	West inlet (tap water) (LPS)	North outlet (LPS)	East outlet (LPS)
Lab-16	2.50	2.00	3.00	1.50
Lab-17	2.50	2.00	2.50	2.00
Lab-18	2.50	2.00	2.25	2.25
Lab-19	2.50	2.00	2.00	2.50
Lab-20	2.50	2.00	1.50	3.00
Lab-21	3.00	1.50	3.00	1.50
Lab-22	3.00	1.50	2.50	2.00
Lab-23	3.00	1.50	2.25	2.25
Lab-24	3.00	1.50	2.00	2.50
Lab-25	3.00	1.50	1.50	3.00

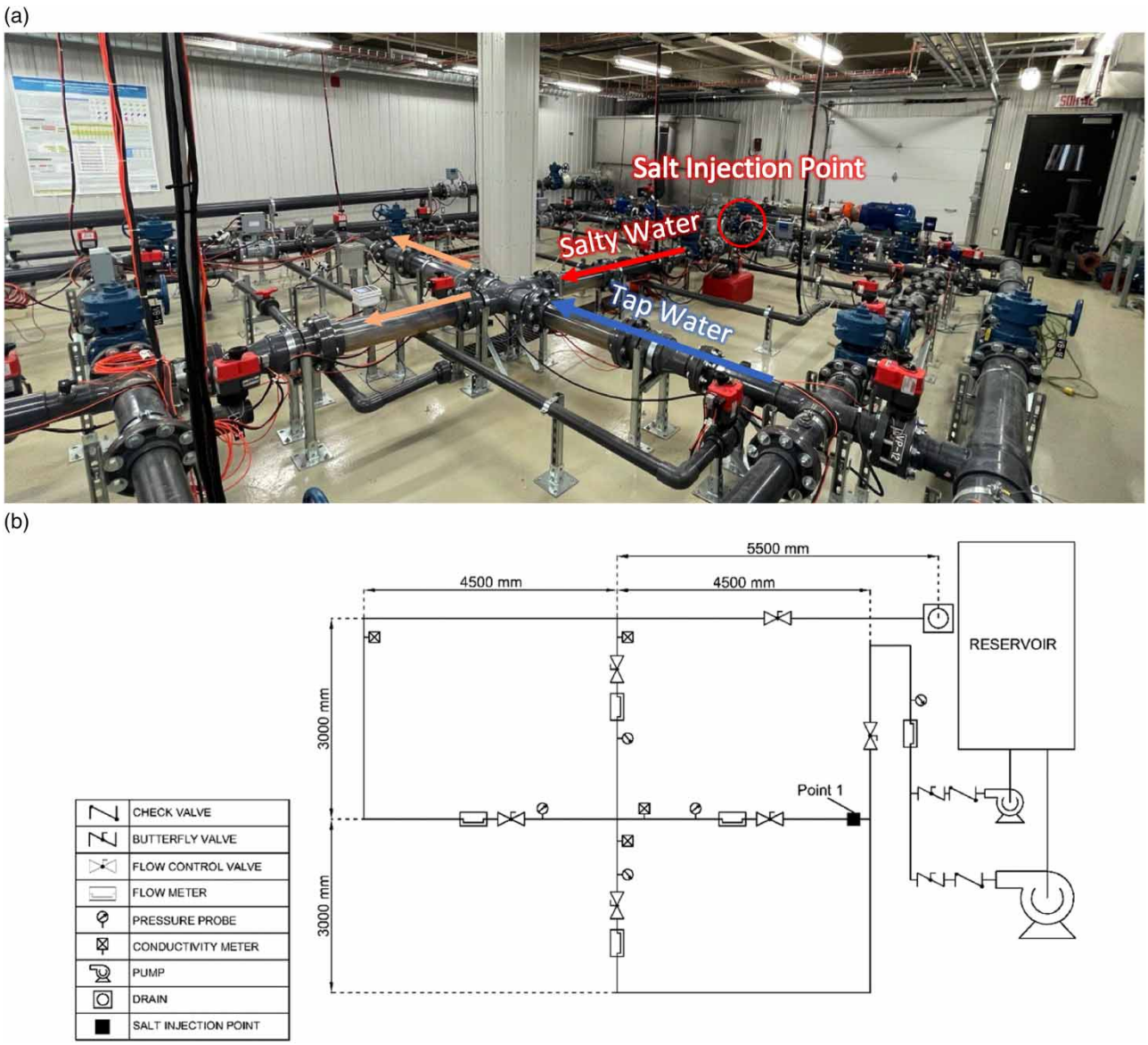

Figure 2 | Laboratory experiments setup: (a) picture of the laboratory and (b) laboratory experimental set-up plan.

and four conductivity meters (Teledyne-LXT220) were installed to measure the conductivity (related to the concentration of salts) in each inlet and outlet. All the settings of pumps and valves were set through a central computer and a control panel designed by Honeywell (Honeywell-EBI R430 and Honeywell-Controller HC900). The measured flow, pressure, and conductivity values were recorded every 5 s. However, in order to reduce the signal noise of the sensors, the measurements were averaged over 60 s intervals.

Tap water was used in the whole network and the injection of a soluble tracer (salt; NaCl) into the network was carried out through a pulse (or an injection) pump. The distance between the salt injection point and the cross junction was about 3 m in all configurations to ensure that longitudinal mixing occurred entirely in water before reaching the cross junction (Figure 2(b)). In all laboratory experiments, the solution of salt was injected into the southern pipe (red arrow in Figure 2(a)), tap water was flowing in the western pipe (blue arrow in Figure 2(a)), and the northern and eastern pipes were the outlets (orange arrows in Figure 2(a)). In each cross junction configuration (Table 1) and for all flow scenarios of the laboratory experiments (Tables 2 and 3), the mixing phenomenon was investigated for two pressure values (320 and 430 kPa). Also, for each pressure and flow rate scenario within the cross junction configurations, 10 different concentrations of salt were injected into the southern pipe.

In all experiments, the dimensionless concentration of injected salt in each outlet, which was acquired from Equation (1), was selected to represent the level of mixing:

$$C^* = \frac{C - C_w}{C_s - C_w} \tag{1}$$

where C^* is the dimensionless concentration of injected salt in the studied outlet (north or east), C is the concentration of salt in the studied outlet, C_s is the concentration of salt in the southern (salty water) inlet, and C_w is the concentration of salt in the western (tap water) inlet. Finally, since 10 different quantities of salt were injected for each flow scenario, the dimensionless concentration of injected salt for each cross junction configuration and each flow scenario was obtained by averaging the dimensionless concentration for each of the 10 injected salt quantities (Equation (2)):

$$\overline{C^*} = \frac{\sum_{i=1}^{10} C_i^*}{10} \tag{2}$$

where C_i^* is the dimensionless concentration in any outlet for the ith of 10 experiments carried out in each flow rate scenario. The uncertainty of the dimensionless concentration in any outlet was estimated through the technique of absolute error propagation, leading to a value of about ± 0.05, based on the accuracy of the conductivity meters, which was ± 0.00141 ms/cm.

2.3. CFD simulations

Numerical (CFD) experiments were also carried out to study the mixing phenomenon within the flow scenarios listed in Table 4, which complemented the laboratory experiment flow scenarios (listed in Tables 2 and 3). To do so, the k-epsilon model of OpenFOAM-v2210 within the solver of twoLiquidMixingFoam was used. OpenFOAM-v2210 is an open-source CFD tool using the finite volume method. The solver, twoLiquidMixingFoam, can consider the transport and mixing of two liquids with different specifications. OpenFOAM was selected for CFD simulations because it is an open-source tool. Since OpenFOAM works with the k-epsilon model, this closure model was employed for turbulent modeling. More details about the closure model and the governing equations of this model, as used in OpenFOAM, are presented in Goodarzi *et al.* (2020).

The CFD model was calibrated and validated based on the experimental results of all scenarios displayed in Table 2. The calibration was conducted by adjusting the turbulent Schmidt number value in order to minimize the difference between the dimensionless eastern outlet concentrations obtained from CFD simulations and laboratory observations, for all flow scenarios in Table 2 and all junction configurations in Table 1. Four turbulent Schmidt number values were tested: 0.01, 0.135 (as suggested by Romero-Gomez *et al.* (2008b)), 1.00, and a value adopted from the contour of the fitted turbulent Schmidt number provided by Romero-Gomez *et al.* (2008c). This last value is a function of both the inlet Re number ratio and the outlet Re number ratio.

Table 4 | CFD flow rate scenarios for developing the new IM model

Scenario	South inlet (salty water) (LPS)	West inlet (tap water) (LPS)	North outlet (LPS)	East outlet (LPS)	Scenario	South inlet (salty water) (LPS)	West inlet (tap water) (LPS)	North outlet (LPS)	East outlet (LPS)
CFD-1	0.50	1.00	0.50	1.00	CFD-21	3.00	8.00	9.00	2.00
CFD-2	0.75	1.25	1.25	0.75	CFD-22	3.00	15.00	10.50	7.50
CFD-3	1.00	0.50	1.00	0.50	CFD-23	3.00	30.00	25.50	7.50
CFD-4	1.00	1.00	1.00	1.00	CFD-24	4.00	4.00	2.00	6.00
CFD-5	2.00	0.50	2.00	0.50	CFD-25	4.00	40.00	4.00	40.00
CFD-6	2.00	1.00	1.00	2.00	CFD-26	5.00	3.00	5.00	3.00
CFD-7	2.00	4.00	2.00	4.00	CFD-27	5.00	25.00	5.00	25.00
CFD-8	2.00	6.00	5.00	3.00	CFD-28	6.00	2.00	4.00	4.00
CFD-9	2.00	8.00	6.00	4.00	CFD-29	6.00	4.00	4.00	6.00
CFD-10	2.00	8.00	8.00	2.00	CFD-30	6.00	4.50	1.50	9.00
CFD-11	2.00	12.00	11.00	3.00	CFD-31	10.00	1.00	10.00	1.00
CFD-12	2.00	16.00	14.00	4.00	CFD-32	10.00	2.00	2.00	10.00
CFD-13	2.00	20.00	12.00	10.00	CFD-33	15.00	2.00	7.00	10.00
CFD-14	2.00	40.00	22.00	20.00	CFD-34	20.00	2.00	2.00	20.00
CFD-15	2.00	40.00	32.00	10.00	CFD-35	30.00	1.00	1.00	30.00
CFD-16	2.00	80.00	62.00	20.00	CFD-36	30.00	2.00	12.00	20.00
CFD-17	2.10	8.00	8.10	2.00	CFD-37	38.00	4.00	2.00	40.00
CFD-18	2.50	1.00	2.50	1.00	CFD-38	40.00	1.00	1.00	40.00
CFD-19	3.00	2.00	3.00	2.00	CFD-39	40.00	2.00	2.00	40.00
CFD-20	3.00	7.50	3.00	7.50	CFD-40	79.00	2.00	1.00	80.00

The same fluid specification was considered for contaminated and clean water, namely a density of 1,000 kg/m^3 and a kinematic viscosity of 1.00×10^{-6} m^2/s. The geometry of the junctions was created through SolidWorks (Version 2021), and the snappyHexMesh tool of OpenFOAM was used to generate the mesh. Mesh analysis was carried out, and the final mesh was selected for each configuration from different meshes with a total number of cells in the range of 440,000 to 108,160,000. The boundary conditions applied for these simulations in all CFD experiments are presented in Table 5.

In Table 5, the flowRateInletVelocity and the flowRateOutletVelocity conditions adjust the velocity field to match the specified flow rate. Regarding the fixedValue condition of k and epsilon, the values of these boundary conditions were calculated using Equations (3) and (4), as suggested by Jasak *et al.* (2007) and Launder & Spalding (1974):

$$k = \frac{3}{2}(Iu)^2 \tag{3}$$

$$\text{epsilon} = \frac{C_\mu^{0.75} k^{1.5}}{L} \tag{4}$$

Table 5 | Boundary conditions applied in OpenFOAM for CFD simulations

Variable	Inlets	Outlets	Walls
Velocity	flowRateInletVelocity	flowRateOutletVelocity	noSlip
Pressure	zeroGradient	zeroGradient	zeroGradient
k	fixedValue	zeroGradient	kqRWallFunction
epsilon	fixedValue	zeroGradient	epsilonWallFunction

where I is the turbulence intensity (set as 5%), u is the average velocity of flow (m/s), C_μ is the model constant (set as 0.09 as suggested in Launder & Spalding (1974)), and L is the length scale (m) (set as 3.8% of the pipe diameter as suggested in Launder & Spalding (1974) and Launder & Spalding (1972)). Equations (3) and (4) are also recommended in the user guide of OpenFOAM.

The validation of the CFD model was then conducted by comparing the results of CFD simulations and laboratory experiments for the cross junctions of 100 × 100 × 100 × 100 mm pipe diameters within the 25 flow rate scenarios. Based on mesh analysis and the calibration of the turbulent Schmidt number, the CFD model was validated. Figure 3 shows the validation of the CFD simulation for all 25 flow rate scenarios.

3. RESULTS AND DISCUSSIONS

3.1. CFD model calibration

The laboratory flow scenarios that were used to develop the model (Table 2) were also used to calibrate the transport equation of the twoLiquidMixingFoam solver (the turbulent Schmidt number). Consistent with the research by Romero-Gomez *et al.*

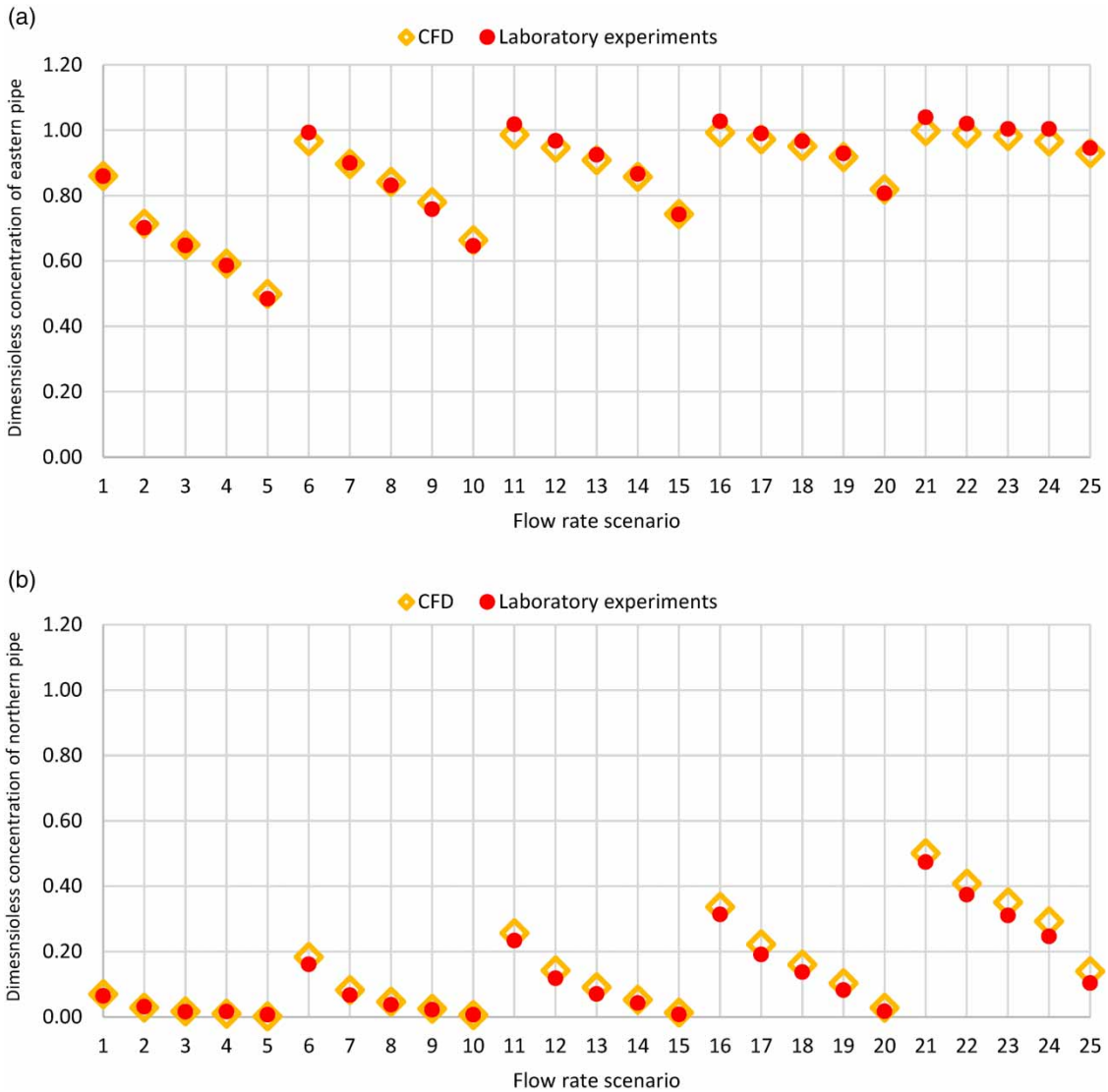

Figure 3 | Results of CFD simulations and laboratory experiments for the cross junction with a pipe diameter of 100 mm in terms of dimensionless concentration of the eastern pipe (a) and dimensionless concentration of the northern pipe (b) within all flow rate scenarios.

(2008b), it was observed in the current study that the CFD simulation results with a turbulent Schmidt number of 0.135 lead to the best agreement with the experimental results. Indeed, the root-mean-squared error (RMSE) between the simulated and observed dimensionless concentrations in the eastern pipe was 0.214, 0.018, 0.326, and 0.029, respectively, for turbulent Schmidt numbers 0.01, 0.135, and 1.00, and the turbulent Schmidt number values adopted from the contour provided by Romero-Gomez *et al.* (2008c). Therefore, a value of 0.135 was assigned to the turbulent Schmidt number for all CFD simulations carried out in this research.

3.2. Principal combinations of independent variables

In order to fit a single regression equation for all studied configurations, an analysis was carried out to find the principal combination of independent variables. The principal combination of independent variables was defined as the one based on which the outlet concentrations could be sorted. Different ratios of inlet and outlet velocities, ratios of inlets and outlet flow rates, and ratios of inlet and outlet Re numbers were taken into account to find the principal combination.

In some IM models, the inlet Re number ratio (Re_s/Re_w) and the outlet Re number ratio (Re_e/Re_n) were taken into account as independent variables (Austin *et al.* 2008; Yu *et al.* 2014b). However, it was observed from our experimental results that these ratios were not the principal combination explaining the mixing behavior (concentrations at the outlets). Indeed, in some cases, the outlet concentrations were different when the inlet Re number ratio and the outlet Re number ratio were the same, as shown in Table 6.

In addition to the inlet and outlet Re number ratios, Shao *et al.* (2014) employed the momentum ratio (η), computed with Equations (5) and (6), as the main parameter explaining the outlet concentrations.

$$\eta = \frac{K_w + K_e}{K_s + K_n} \tag{5}$$

$$K_i = \frac{Q_i^2}{A_i} \tag{6}$$

where K_i is the momentum in the pipe leg i (w = west; e = east; s = south; and n = north), Q_i is the flow rate in the pipe leg i, and A_i is the area of that pipe leg cross section. As for the Re number ratios, it was observed from the experimental results that the momentum ratios were occasionally the same while the outlet concentrations were different, as shown in Table 7.

In EPANET-BAM (Ho 2008) and in the IM model by Hernández Cervantes *et al.* (2021), the inlet flow ratio (Q_s/Q_w) and the outlet flow ratio (Q_e/Q_n) were considered as independent variables. To verify if these ratios could be the principal combination of independent variables explaining the outlet concentrations, the results for the eastern outlet concentrations under the flow scenarios listed in Table 2 are depicted in Figure 4 for configuration D.

Four possibilities of sorting the eastern outlet concentrations as a function of the inlet and outlet flow ratios are illustrated in Figure 4. The other four possibilities for sorting the data are the exact mirrors of these figures. Accordingly, as it can be seen in Figure 4, it is not possible to sort the eastern concentrations in ascending or descending order based on the inlet flow ratio and the outlet flow ratio.

These investigations show that the inlet and outlet Re number ratios, the inlet and outlet flow ratios, and the momentum ratio could hardly be considered as the principal combinations of independent variables explaining the outlet concentrations. However, when the ratio of the eastern pipe flow to the southern pipe flow (Q_e/Q_s) and the ratio of the eastern pipe flow to the western pipe flow (Q_e/Q_w) are taken into account, both outlets' concentrations can be sorted in descending order, as shown in Figure 5, for the eastern outlet of all flow scenarios listed in Table 2. In this figure, first, the concentrations were sorted based on (Q_e/Q_s) in descending order, and then, the concentrations were sorted based on (Q_e/Q_w) in ascending

Table 6 | Counter example for considering inlet and outlet *Re* number ratios as the principal combination

Configuration	Flow scenario	Re_s/Re_w	Re_e/Re_n	$\overline{C_e^*}$	$\overline{C_n^*}$
A	Lab-3	0.50	1.00	0.70	0.03
E	Lab-5	0.50	1.00	0.49	0.01
F	Lab-1	0.50	1.00	0.88	0.07

Table 7 | Counter example for considering the momentum ratio

Configuration	Flow scenario	η	$\overline{C_e^*}$	$\overline{C_n^*}$
A	Lab-3	387,321,135.73	0.70	0.03
A	Lab-10	387,321,135.73	0.78	0.02
D	Lab-3	884,601,355.69	0.65	0.02
D	Lab-10	884,601,355.69	0.74	0.01

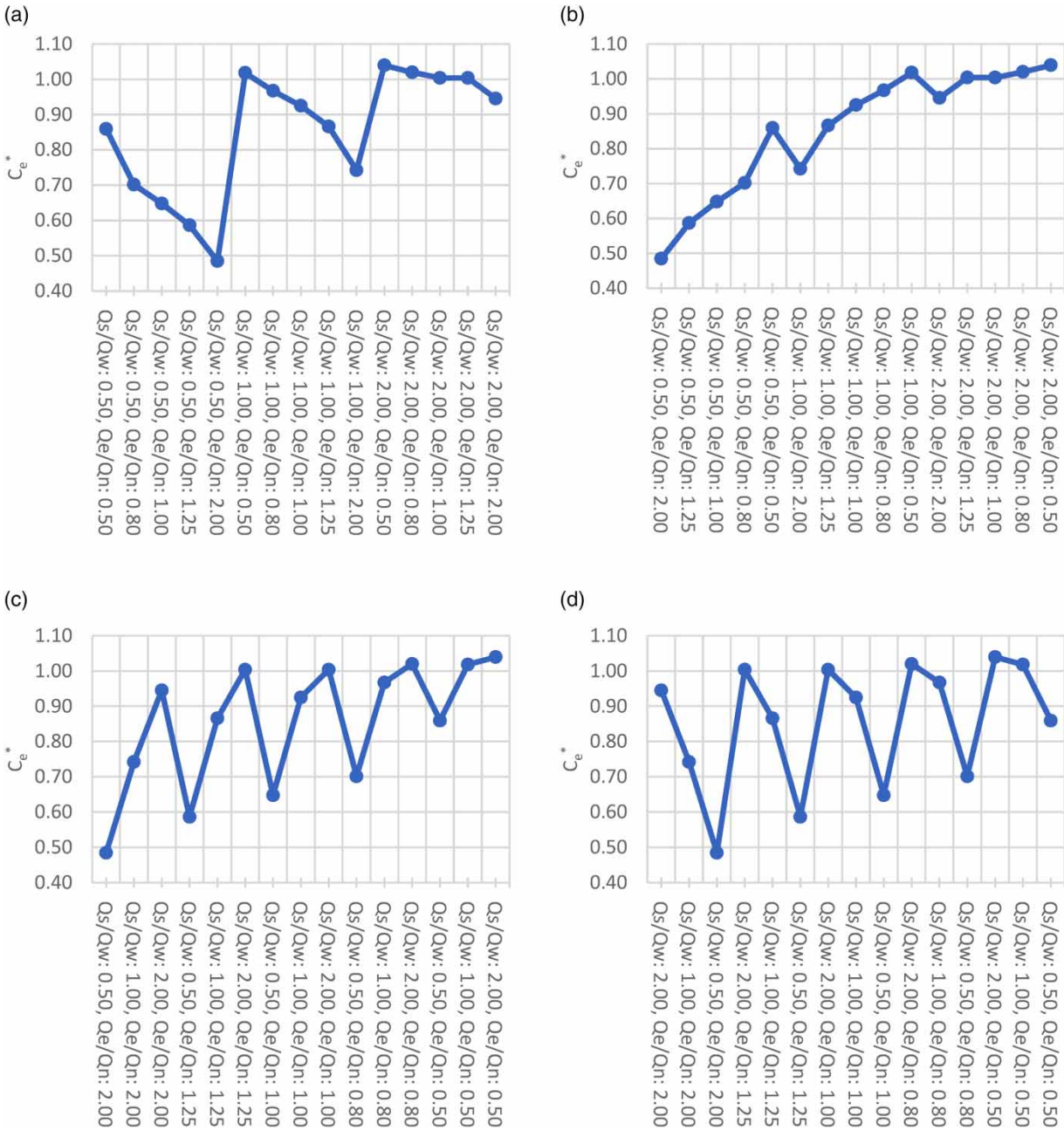

Figure 4 | Eastern dimensionless concentration as a function of inlet and outlet flow ratios: (a) inlet flow ratio descending, outlet flow ratio descending; (b) inlet flow ratio descending, outlet flow ratio ascending; (c) outlet flow ratio ascending, inlet flow ratio descending; (d) outlet flow ratio ascending, inlet flow ratio ascending.

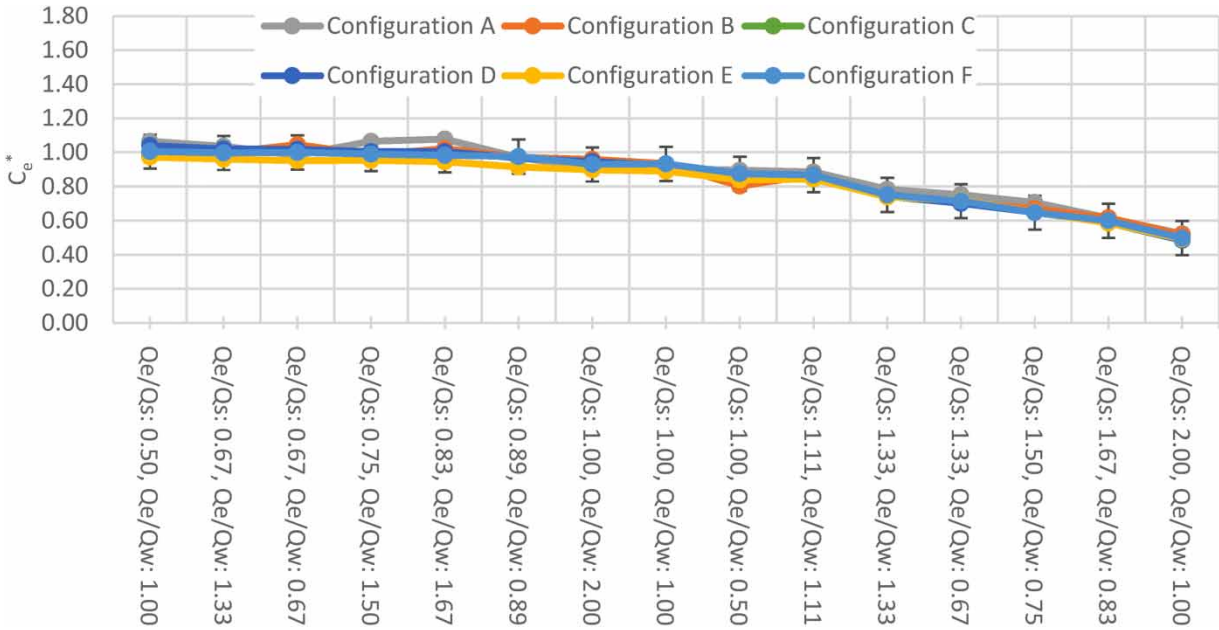

Figure 5 | Eastern dimensionless concentration as a function of flow ratios of eastern pipe to southern pipe and of eastern pipe to western pipe, sorted in the descending and ascending order, respectively, for flow scenarios Lab-1 to Lab-15.

order for the same (Q_e/Q_s) ratios. The error bars in Figure 5 represent the uncertainty of the laboratory experiments (5.0%), which comes from the uncertainty of flow and conductivity measurements.

It is observed in Figure 5 that for all studied configurations, when the ratios of (Q_e/Q_s) and (Q_e/Q_w) are the same, the dimensionless concentrations in the eastern pipe (mixing behavior) are similar. Therefore, those two flow ratios of the eastern pipe to the southern pipe and of the eastern pipe to the western pipe were used as independent variables in the IM model developed in this study.

3.3. Mixing model development

To avoid using a calibration parameter (like the scaling parameter in EPANET-BAM) and to reduce the calculation time of water quality models with IM, a single regression equation was fitted on experimental results. The equation was developed based on the laboratory flow scenarios listed in Table 2 and on the CFD results for flow scenarios listed in Table 4, for all studied configurations, to estimate the dimensionless concentration in the eastern outlet (Equations (7) and (8)):

$$\text{for } Q_e/Q_s \leq 0.85\text{: } C_e^* = 1.00 \tag{7}$$

$$\text{for } Q_e/Q_s > 0.85\text{: } C_e^* = 0.022 \times \ln\left(\frac{Q_e}{Q_s}\right) + 0.91 \times \left(\frac{Q_e}{Q_w}\right)^{-0.79} \tag{8}$$

The dimensionless concentration in the northern outlet can then be calculated based on the mass balance equation (Equation (9)):

$$C_n^* = \frac{(C_s^* Q_s - C_e^* Q_e)}{Q_n} \tag{9}$$

These last equations have some limitations which should be taken into account before employing them. First, the equations work only for cross junctions within the six studied configurations. The pipe diameters of cross junctions in laboratory experiments were 150 mm or less and, therefore, the proposed equations can be used for cross junctions within the pipe diameter range of 50 to 150 mm. The flow rates tested to develop this equation were between 0.50 and 80.00 LPS and the ratios (Q_e/Q_s)

and (Q_e/Q_w) were between 0.50 and 40.00; it is recommended that the proposed equations are used for the same range of flow rates.

3.4. Mixing model validation

The RMSE was selected as a performance indicator since it is one of the most commonly used measures to show how far predictions fall from observation values. The RMSE between the simulated and observed dimensionless concentrations in the eastern outlet for the flow scenarios of the developing data set (Tables 2 and 4) is 0.027, while it is 0.015 for the flow scenarios of the validation data set (Table 3). Those results are illustrated in Figure 6. The error bars in this figure show the uncertainty of the laboratory experiments (5.0%). As can be seen in Figure 6, the results of the validation data set, considering the uncertainties of measurements, are all around the 1:1 line. The results presented in Figure 6 and the RMSE values mentioned above confirm that the dimensionless concentrations computed with the developed model are in good agreement with the observations.

3.5. Comparison of developed mixing model with existing models

According to Yousefian (2023), AZRED (Austin *et al.* 2008) and the IM model by Shao *et al.* (2014) are the two existing IM models that provide the best estimates of outlet concentrations under real-world conditions. Besides, these two models are not dependent on a scaling parameter as EPANET-BAM is. However, these models were only developed for junctions with equal leg sizes, as encountered in configurations A and D (more details of these IM models are provided in the supplementary materials). Therefore, the results of these two models are compared to those of the newly developed mixing model for configurations A and D, and for all flow scenarios of the laboratory experiments (listed Tables 2 and 3) in Figure 7. This figure shows the distribution of the absolute difference between the C_e^* values computed by each model and the $\overline{C_e^*}$ values obtained from the laboratory experimental results. The quartiles of errors are shown by the three lines in each box of Figure 7. The lower and higher range limits of the bars were calculated based on Equations (10) and (11):

$$\text{lower range limit} = Q_1 - 1.5 \times (Q_3 - Q_1) \tag{10}$$

$$\text{higher range limit} = Q_3 + 1.5 \times (Q_3 - Q_1) \tag{11}$$

where Q_1 is the first quartile and Q_3 is the third quartile.

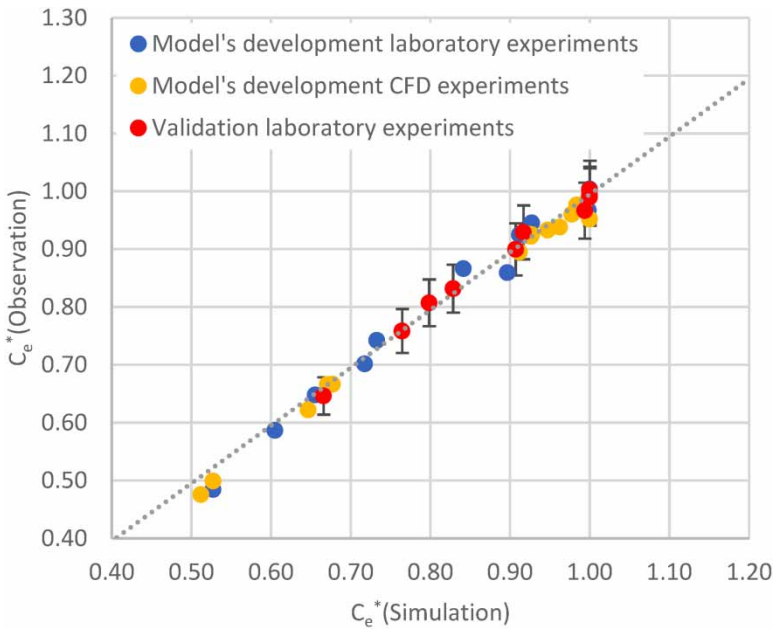

Figure 6 | Results of the simulated and observed concentrations in the eastern outlet.

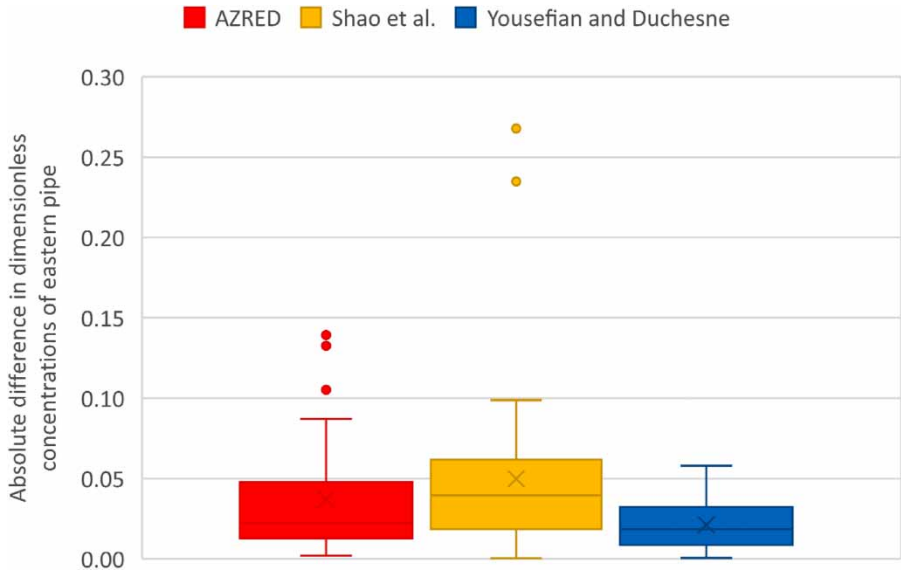

Figure 7 | Absolute difference between the experimental results and the results of the IM models, in terms of dimensionless concentration in the eastern pipe.

Figure 7 shows that the newly developed model leads to the least differences between the observed and computed concentrations. It is also observed that, for the studied flow scenarios, the model developed in this study does not have any outlier, while some are present in the results of the AZRED model and the IM model by Shao *et al.* (2014). The RMSE between the simulated and observed concentrations of the eastern pipe, for configurations A and D, is 0.02 for the newly developed model, while it is of 0.05 and 0.07, respectively, for the AZRED model and the IM model by Shao *et al.* (2014).

This newly developed equation can be integrated into EPANET to improve water quality modeling in real-world water distribution systems. The current EPANET model with complete mixing assumption leads, in some cases, to errors in applications of water quality simulations such as water age modeling, disinfectant residual modeling, and water quality sensor placement. Although there are some existing IM models that can improve the accuracy of water quality modeling, they were developed and applied only on a limited number of junction types. However, the newly developed equation could reduce this limitation by considering more types of junctions, such as cross junctions with real-world pipe diameters and cross junctions with different pipe diameters.

4. CONCLUSIONS

The mixing phenomenon was studied at cross junctions with equal and unequal pipe sizes. Laboratory experiments were conducted under real-world conditions, such as 100 and 150 mm pipe sizes. Besides, OpenFOAM was calibrated and employed to simulate mixing under flow scenarios complementing the laboratory-tested flow scenarios.

Most existing models with IM were developed within laboratory conditions (i.e., pipe sizes smaller than in real-world networks) and for junctions with equal pipe sizes. Some models developed for junctions with unequal pipe sizes either depend on predetermined parameters, like the scaling parameter of EPANET-BAM-WRAP, or work with only limited pipe size ratios, like 25/32 and 25/50 in the analytical model by Yu *et al.* (2014b). This study investigated real-world cross junction sizes, such as 150 × 100 × 150 × 100 mm and 100 × 150 × 150 × 150 mm, which no existing IM model can simulate. A single equation was proposed to compute outlets' concentrations for all considered junctions' configurations. Based on the obtained results, it can be concluded that

1. For the studied junction configurations and flow rate scenarios, a Schmidt number of 0.135 showed the best agreement between outlets' concentrations obtained from laboratory experiments and numerical simulations.
2. The outlet concentrations could not be sorted in ascending or descending order for any of the following ratios: inlet Re number ratio and outlet Re number ratio, inlet flow rate ratio and outlet flow rate ratio, and the momentum ratio (defined by Shao *et al.* (2014)).

3. The outlet concentrations could be sorted in ascending or descending order, as a function of the ratio of the flow rate of the eastern pipe to the flow rate of the southern pipe and of the ratio of the flow rate of the eastern pipe to the flow rate of the western pipe; those two ratios were thus used to compute the outlet concentrations in the developed model.
4. The outlet concentrations computed by the developed model are closer to observations than those computed by two other IM models, namely AZRED and the IM model by Shao *et al.* (2014).

Although the developed model in this study could work for a broader range of junction configurations, it is recommended to be used with flow rates between 0.50 and 80.00 LPS and flow rate ratios between 0.5 and 40. Besides, it is important to emphasize that the findings of this study are also subject to some limitations. First, the pipe sizes were limited to 150 mm or less. Second, cross junctions with unequal pipe sizes were installed using fittings for laboratory experiments. Third, the flow rates in laboratory experiments were limited to 1.50 and 3.00 LPS. Therefore, some issues need to be investigated in the future. Indeed, the principal combinations of independent variables identified in this research should be evaluated for other junctions' types and configurations (e.g., double-tee junctions, other cross junction sizes, etc.). Nevertheless, the developed model and the future proposed research of this study could improve water quality models in order to increase the use in disinfectant residual management, water quality simulations in WDNs with different water sources, water quality sensor placement, and contaminant source identification.

ACKNOWLEDGEMENTS

The authors would like to thank Mr Pierre-Olivier Schwarz and Mr Laurent Émond for their precious help in conducting this research. This research was funded by the Natural Sciences and Engineering Research Council of Canada, Grant No. RGPIN-2018-05473.

DATA AVAILABILITY STATEMENT

All relevant data are included in the paper or its Supplementary Information.

CONFLICT OF INTEREST

The authors declare there is no conflict.

REFERENCES

Ashgriz, N., Brocklehurst, W. & Talley, D. 2001 Mixing mechanisms in a pair of impinging jets. *Journal of Propulsion and Power* **17**, 736–749.

Austin, R., Van Bloemen Waanders, B., Mckenna, S. & Choi, C. Y. 2008 Mixing at cross junctions in water distribution systems. II: Experimental study. *Journal of Water Resources Planning and Management* **134**, 295–302.

BENTLEY SYSTEMS. 2020 *WaterGEMS User's Guide*. Bentley Systems Inc, Exton, PA, USA.

Braun, M., Bernard, T., Ung, H., Piller, O. & Gilbert, D. 2015 Computational fluid dynamics modeling of contaminant mixing at junctions for an online security management toolkit in water distribution networks. *Journal of Water Supply: Research and Technology – AQUA* **64**, 504–515.

Choi, C. Y., Shen, J. Y. & Austin, R. G. 2008 Development of a comprehensive solute mixing model (AZRED) for double-tee, cross, and wye junctions. In: *Water Distribution Systems Analysis 2008* (Kobus V. Z., ed.). American Society of Civil Engineers, Kruger National Park, South Africa, pp. 1–10.

Cotes, L., Saldarriaga, J. & Bohórquez, J. 2016 Physical and computational modeling of mixing processes in potable water network junctions. In *World Environmental and Water Resources Congress 2016*, May 22–26 2016, West Palm Beach, FL, USA. American Society of Civil Engineers, pp. 531–541.

Fowler, A. G. & Jones, P. 1991 Simulation of water quality in water distribution systems. In *Proceedings of Water Quality Modeling in Distribution Systems*. AwwaRF/EPA, Cincinnati, OH, USA.

Gilbert, D., Mortazavi, I., Piller, O. & Ung, H. 2017 Low dimensional modeling of Double T-junctions in water distribution networks using Kriging interpolation and Delaunay triangulation. *Pacific Journal of Mathematics for Industry* **9**, 1–19.

Goodarzi, D., Abolfathi, S. & Borzooei, S. 2020 Modelling solute transport in water disinfection systems: Effects of temperature gradient on the hydraulic and disinfection efficiency of serpentine chlorine contact tanks. *Journal of Water Process Engineering* **37**, 101411.

Grbčić, L., Kranjčević, L., Družeta, S. & Lučin, I. 2020a Efficient double-tee junction mixing assessment by machine learning. *Water* **12**, 238–254.

Grbčić, L., Kranjčević, L., Lučin, I. & Sikirica, A. 2020b Large Eddy simulation of turbulent fluid mixing in double-tee junctions. *Ain Shams Engineering Journal* **12**, 789–797.

Hammoudi, H. 2021 *Modeling of Mixing in Cross Junction Using Computational Fluid Dynamics. Ph.D.*, Technische Universitat Dresden.

Hernández Cervantes, D., Delgado Galván, X., Nava, J. L., López Jiménez, P. A., Rosales, M. & Mora Rodríguez, J. 2018 Validation of a computational fluid dynamics model for a novel residence time distribution analysis in mixing at cross-junctions. *Water* **10**, 733–751.

Hernández Cervantes, D., López-Jiménez, P. A., Nevárez, J. A. A., Delgado Galván, X., Jiménez Magaña, M. R., Pérez-Sánchez, M. & De Jesús Mora Rodríguez, J. 2021 Incomplete mixing model at cross-junctions in EPANET by polynomial equations. *Water* **13**, 453.

Ho, C. K. 2008 Solute mixing models for water-distribution pipe networks. *Journal of Hydraulic Engineering* **134**, 1236–1244.

Ho, C. K. & Khalsa, S. S. 2008 EPANET-BAM: Water quality modeling with incomplete mixing in pipe junctions. In: *Water Distribution Systems Analysis 2008*. American Society of Civil Engineers, Kruger National Park, South Africa.

Ho, C. K. & O'rear Jr, L. 2009 Evaluation of solute mixing in water distribution pipe junctions. *Journal-American Water Works Association* **101**, 116–127.

Ho, C. K., O'rear Jr, L., Wright, J. L. & Mckenna, S. A. 2006 Contaminant mixing at pipe joints: Comparison between laboratory flow experiments and computational fluid dynamics models. In: *Water Distribution Systems Analysis Symposium* (Kobus V. Z., ed.), August 27–30, 2006, Cincinnati, OH, USA. American Society of Civil Engineers, pp. 1–18.

Ho, C. K., Choi, C. Y. & Mckenna, S. A. 2007 Evaluation of complete and incomplete mixing models in water distribution pipe network simulations. In: *World Environmental and Water Resources Congress 2007: Restoring Our Natural Habitat*, May 15–19 2007, Tampa, Florida, USA. American Society of Civil Engineers, pp. 1–12.

Jasak, H., Jemcov, A. & Tukovic, Z. 2007 OpenFOAM: A C ++ library for complex physics simulations. *International Workshop on Coupled Methods in Numerical Dynamics*, 2007. IUC Dubrovnik Croatia, pp. 1–20.

Launder, B. E. & Spalding, D. B. 1972 Mathematical Models of Turbulence. *Journal of Fluid Mechanics* **57** (4), 826–828. https://doi.org/10.1017/S0022112073222048.

Launder, B. E. & Spalding, D. B. 1974 The numerical computation of turbulent flows. *Computer Methods in Applied Mechanics and Engineering* **3**, 269–289.

Mckenna, S. A., Orear, L. & Wright, J. 2007 Experimental determination of solute mixing in pipe joints. In *World Environmental and Water Resources Congress 2007: Restoring Our Natural Habitat*, May 15–19, 2007, Tampa, FL, USA. American Society of Civil Engineers, pp. 1–11.

Mckenna, S. A., O'hern, T. & Hartenberger, J. 2008 Detailed investigation of solute mixing in pipe joints through high speed photography. In: *Water Distribution Systems Analysis 2008* (Kobus V. Z., ed.). August 17–20, 2008. American Society of Civil Engineers, Kruger National Park, South Africa, pp. 1–12.

Mompremier, R., Pelletier, G., Fuentes Mariles, Ó. A. & Ghebremichael, K. 2015 Impact of incomplete mixing in the prediction of chlorine residuals in municipal water distribution systems. *Journal of Water Supply: Research and Technology-Aqua* **64**, 904–914.

Mompremier, R., Fuentes Mariles, Ó. A., Silva Martínez, A. E., Becerril Bravo, J. E. & Ghebremichael, K. 2017 Impact of mixing phenomenon at cross junctions on the variation of total coliform and *E. coli* in water distribution systems: Experimental study. *Journal of Water Supply: Research and Technology – AQUA* **66**, 308–318.

Orear, L., Hammond, G., Mckenna, S. A., Molina, P., Johnson, R., O'hern, T. & Van Bloemen Waanders, B. 2005 *Physical Modeling of Scaled Water Distribution System Networks*. USDOE (U.S. Department of Energy Office of Scientific and Technical Information): Sandia National Lab. (SNL-NM), Albuquerque, NM, USA.

Romero-Gomez, P. & Choi, C. Y. 2011 Axial dispersion coefficients in laminar flows of water-distribution systems. *Journal of Hydraulic Engineering* **137**, 1500–1508.

Romero-Gomez, P., Choi, C. Y., Lansey, K. E., Preis, A. & Ostfeld, A. 2008a Sensor network design with improved water quality models at cross junctions. In: *Water Distribution Systems Analysis 2008* (Kobus V. Z., ed.). August 17–20, 2008a. American Society of Civil Engineers, Kruger National Park, South Africa, pp. 1–9.

Romero-Gomez, P., Choi, C. Y., Van Bloemen Waanders, B. & Mckenna, S. 2008b Transport phenomena at intersections of pressurized pipe systems. In: *Water Distribution Systems Analysis Symposium 2006* (Steven, G. B., Robert, M. C., Walter, M. G., James, G. U., eds.). American Society of Civil Engineers, Cincinnati, OH, USA.

Romero-Gomez, P., Ho, C. K. & Choi, C. Y. 2008c Mixing at cross junctions in water distribution systems. I: Numerical study. *Journal of Water Resources Planning and Management* **134**, 285–294.

Rossman, L. A. 2000 *EPANET 2: User's Manual*. U.S. Environmental Protection Agency, Cincinnati, OH, USA.

Shao, Y., Yang, Y. J., Jiang, L., Yu, T. & Shen, C. 2014 Experimental testing and modeling analysis of solute mixing at water distribution pipe junctions. *Water Research* **56**, 133–147.

Shao, Y., Zhao, L., Yang, Y. J., Zhang, T. & Ye, M. 2019 Experimentally determined solute mixing under laminar and transitional flows at junctions in water distribution systems. *Advances in Civil Engineering* **2019**, 1–10.

Solidworks, D. S. Version 2021. SolidWorks®.

Song, I., Romero-Gomez, P. & Choi, C. Y. 2009 Experimental verification of incomplete solute mixing in a pressurized pipe network with multiple cross junctions. *Journal of Hydraulic Engineering* **135**, 1005–1011.

Song, I., Romero-Gomez, P., Andrade, M. A., Mondaca, M. & Choi, C. Y. 2018 Mixing at junctions in water distribution systems: An experimental study. *Urban Water Journal* **15**, 32–38.

Ung, H. 2016 *Quasi Real-Time Modeling for Security of Water Distribution Network*. *Ph.D. Thesis*, Université de Bordeaux.

Ung, H., Piller, O. & Denis, G. 2014 Quasi-real time modeling for security of a drinking water distribution network. *Procedia Engineering* **70**, 800–809.

Van Summeren, J., Meijering, S., Beverloo, H. & Van Thienen, P. 2017 Design of a distribution network scale model for monitoring drinking water quality. *Journal of Water Resources Planning and Management* **143**, 04017051(1)–04017051(10).

Webb, S. W. 2007 High-fidelity simulation of the influence of local geometry on mixing in crosses in water distribution systems. In: *World Environmental and Water Resources Congress 2007* (Karen C. K., ed.). Restoring Our Natural Habitat, May 15–19, 2007. American Society of Civil Engineers, Tampa, FL, USA, pp. 1–14.

Webb, S. W. & Van Bloemen Waanders, B. G. 2006 High fidelity computational fluid dynamics for mixing in water distribution systems. In: *Water Distribution Systems Analysis Symposium*, August 27–30, 2006, Cincinnati, OH, USA. American Society of Civil Engineers, pp. 1–15.

Yousefian, R. & Duchesne, S. 2022a *Experimental Study of Mixing Phenomenon in Water Distribution Networks Under Real-World Conditions*. WDSA/CCWI 2022, Valencia, Spain.

Yousefian, R. & Duchesne, S. 2022b Modeling the mixing phenomenon in water distribution networks: A state-of-the-Art review. *Journal of Water Resources Planning and Management* **148**, 03121002(1)–03121002(12).

Yousefian, R. 2023 *Improving Water Quality models for Contamination Source Identification in Drinking Water Distribution Networks. Ph.D. Thesis,* Institut National de la Recherche Scientifique, Canada.

Yu, T., Tao, L., Shao, Y. & Zhang, T. 2014a Experimental study of solute mixing at double-Tee junctions in water distribution systems. *Water Science and Technology: Water Supply* **15**, 474–482.

Yu, T. C., Shao, Y. & Shen, C. 2014b Mixing at cross joints with different pipe sizes in water distribution systems. *Journal of Water Resources Planning and Management* **140**, 658–665.

Yu, T., Qiu, H., Yang, J., Shao, Y. & Tao, L. 2016 Mixing at double-Tee junctions with unequal pipe sizes in water distribution systems. *Water Science and Technology: Water Supply* **16**, 1595–1602.

First received 21 February 2023; accepted in revised form 21 December 2023. Available online 18 January 2024